Aerosol Science and Technology
Publication details, including instructions for authors and subscription information:
http://www.informaworld.com/smpp/title~content=t713656376

System for Precise Control of Volumetric Flow Rate during Sampling with a Cascade Impactor

Polina Borgoul Maciejczyk [a]; Christopher Kidwell [a]; J. M. Ondov [a]
[a] Department of Chemistry and Biochemistry, University of Maryland, College Park, Maryland.

First Published on: 01 April 2002
To cite this Article: Maciejczyk, Polina Borgoul, Kidwell, Christopher and Ondov, J. M. , (2002) 'System for Precise Control of Volumetric Flow Rate during Sampling with a Cascade Impactor', Aerosol Science and Technology, 36:4, 397 - 406
To link to this article: DOI: 10.1080/027868202753571223
URL: http://dx.doi.org/10.1080/027868202753571223

Aerosol Science and Technology 36: 397–406 (2002)

Published by Taylor and Francis
0278-6826/02/$12.00 + .00

System for Precise Control of Volumetric Flow Rate during Sampling with a Cascade Impactor

Polina Borgoul Maciejczyk, Christopher Kidwell, and J. M. Ondov
Department of Chemistry and Biochemistry, University of Maryland, College Park, Maryland

Calculations were made with efficiency curves developed for the micro-orifice impactor (MOI) to estimate errors in mass collected on individual stages due to fluctuations in the flow rate during sampling of submicrometer particles. The sizes of these errors depend on the size distribution of the sampled aerosol and the level of flow rate fluctuation. For a log-normally distributed particle population, mass errors due to flow rate fluctuations were bimodally distributed about stages with cutpoints near the aerosol Mass Median Aerodynamic Diameter (MMAD). The largest errors occurred uniformly on the stage with the smallest cutpoint (here, 0.059 μm). These errors were asymmetric with respect to sign, which leads to a net error for a randomly fluctuating flow rate. In general, mass errors increased with decreasing geometric standard deviation (σ_g) and were substantially greater for populations with 0.5 μm MMADs than for those with 0.2 μm MMADs. The largest net errors for the former were 4, 110, and 560% for σ_g of 1.2 and flow rate fluctuations of $\pm$1, $\pm$5, and $\pm$10%, respectively, but decreased to 0.03, 0.9, and 4%, respectively, for a σ_g of 1.9. Flow rate fluctuations, therefore, lead to a positive bias in the geometric standard deviation inferred from the measured masses and reduce the user's ability to interpret differences in size distributions. To minimize these effects, we developed and tested a system for controlling the volumetric sampling rate through a MOI at 30 LPM with a precision of 0.06% (600 ms averaging; 0.67% for 5 ms averaging), a level of precision that allows for accurate relative calibration between flow systems and for which errors from flow rate fluctuations are reduced to <1%, even for a very narrow aerosol (σ_g 1.2). Mass errors for an uncontrolled field test were as large as −60%, but these were reduced to <0.22% in a comparable controlled field test. In two replicate tests of the system, agreements between stage masses collected on MOI stage 7 (D_{50} = 0.173 μm) of two simultaneously operated flow-controlled impactors sampling 0.2 μm diameter monodisperse test particles were 0.997 and 0.996, although differences as large as 4% were observed for some stages. The system is suitable for use with standard "Federal Reference Method" samplers.

Received 15 November 1999; accepted 29 June 2001.
Funding for this project was provided by the U.S. Environmental Protection Agency under contract no. R825247010.
Address correspondence to John M. Ondov, Department of Chemistry and Biochemistry, University of Maryland, College Park, MD 20742. E-mail: jondov@wam.umd.edu

INTRODUCTION

Cascade impactors have been widely used for more than 55 years for aerodynamic sizing (May 1945) and to provide size-segregated particulate samples for gravimetric, chemical, and various physical (e.g., surface area) analyses. In addition to permitting determination of size distributions of aerosol properties, impactor measurements are used in combination with other measurements to infer size-dependent aerosol behavior, e.g., deposition velocities (Lin et al. 1994; Caffrey et al. 1998; Hoff et al. 1998). Changes in size distributions of mass and various constituent species have been used to infer temporal characteristics (Annegarn 1983), particle deposition gradients (Paode et al. 1998), atmospheric growth laws (Hering and Friedlander 1982; McMurry and Wilson 1983), hygroscopic growth (Ahlberg and Winchester 1978; Koutrakis et al. 1989; Divita et al. 1995; Divita et al. 1996; Hitzenberger et al. 1997), and atmospheric transformations and secondary aerosol formation processes (McMurry and Wilson 1983; John et al. 1990; Venkataraman and Friedlander 1994; Berner et al. 1996). The sensitivity to which such information can be inferred, however, depends on the ability to accurately determine changes in mass observed on the various impactor stages and, thus, on noise and bias errors in sampling and on measurement uncertainties. Bias errors arise from cross sensitivity (Natusch and Wallace 1976); i.e., departure from ideal collection efficiency curves for each stage, particle bounce and reentrainment (Dzubay et al. 1976; Rao and Whitby 1978; Nurtan et al. 1978; Ondov et al. 1978), wall losses (Cushing et al. 1979), and, as described below, fluctuations in the flow rate during sampling.

For a well-calibrated impactor, cross sensitivity effects are reduced through the use of inversion algorithms that include functions for the efficiency curves of the various stages (Raabe 1978; Dzubay and Hasan 1990; Wolfenbarger and Seinfeld 1990). Particle bounce and reentrainment is reduced by coating impaction stages, especially those used to collect hard, dry particles such as mineral dust present in supermicrometer atmospheric particles; by minimizing the particle velocity required for inertial separation (Kuhlmey et al. 1981); and by the use of rotating stages (Marple et al. 1981).

In impactors, both the aerodynamic diameter of the particle collected with an efficiency of 50% (D_{50}) and the shape of the particle collection efficiency curve depend on the velocity to which particles are accelerated and thus the volumetric sampling flow rate. Clearly, any changes in the flow rate experienced during sampling will broaden the range of particles collected on each stage and reduce the discriminating power of the measurement. But as discussed by Fegley and Ensor (1975), even random fluctuations in the volumetric flow rate will cause broadening and loss of discriminating power, as they lead to errors in the mass collected. Errors in mass collected on an impactor stage arising from flow rate fluctuations should be especially important for stages for which mass is asymmetrically distributed about the adjacent stages, e.g., in the "wings" of a lognormal distribution. In such a case, more mass would be deposited on the center stage when the flow rate shifts in one direction than would be deposited for the opposite direction.

Herein, we discuss error derived from fluctuations in the flow rate during sampling with a micro-orifice impactor (MOI), a popular, moderate flow rate impactor, in which jet velocities and pressure drops are kept low through the use of numerous small jets and for which wall losses and calibration curves have been well characterized (Marple et al. 1991). In addition we describe a system for controlling the sampling rate through a 10 stage MOI at 30 LPM with a precision of 0.06–0.14% in laboratory and field tests, respectively. Model results for a range of positive and negative deviations are given to define the extent of fluctuation errors. Then calculations are presented for actual uncontrolled and controlled flow rate tests with the MOI.

METHODS AND RESULTS

Error from Flow Rate Fluctuations

Errors associated with fluctuations in the volumetric flow rate were computed as the differences between the mass fractions (M_i) of various aerosol populations collected on individual stages of a 9 stage MOI for which efficiency curves were calculated at a target (30 L min^{-1}) and perturbed flow rates of ±0.06, 0.5, 1, 5, and 10%. Additional calculations were made with the actual flow rate data described below. Test aerosol inputs for the simulations included a series of populations generated with a log-normal distribution function (LNDF), f_j, i.e.,

$$f_j = \frac{1}{\ln \sigma_g \ \text{mmad} \ \sqrt{2\pi}} \exp^{-\frac{1}{2}\left(\frac{\ln dp - \ln \text{mmad}}{\ln \sigma_g}\right)^2}, \qquad [1]$$

where f_j is the LNDF for the jth aerosol particle population, d_p is aerodynamic particle diameter, and σ_g and mmad are the geometric standard deviation and mass median aerodynamic diameter of the distribution function written in terms of the linear size interval. Calculations were made for unimodal distributions with mmads of 0.2 and 0.5 μm: the former with σ_gs of 1.2 and 1.45, the latter with σ_gs of 1.2, 1.45, and 1.9. These are representative of fresh accumulation aerosol from controlled sources and aged accumulation aerosol bearing secondary mass (Ondov and Wexler 1998).

Collection efficiency data suitable for individual stages (i, where $i = 0$ for the inlet stage, see Table 1) of each of the impactors were obtained from the University of Minnesota (Marple et al. 1991) and were fit with the sigmoidal function, $\varepsilon_{i,dp}$, of Hasan and Dzubay (1987). Parameters used to describe the impactor efficiency curves used, herein, are reported by Ondov and Divita (1993) and are listed in Table 1. These parameters include the D_{50}, minimum ($\varepsilon_{\min}$) and maximum ($\varepsilon_{\max}$) efficiencies, slope (S), and skew (SK) as defined by (Hasan and Dzubay 1987)

$$\varepsilon_{i,dp} = \varepsilon_{\max_i}\left(\varepsilon_{\min_i} + \frac{(1 - \varepsilon_{\min_i})}{1 + \left(\frac{d_{50,i}}{dp_i}\right)^B}\right), \qquad [2a]$$

where

$$B = S \cdot \left(1 + SK \cdot \left(\frac{dp_i - d_{50,i}}{d_{50,i}}\right)\right). \qquad [2b]$$

Table 1
Stage D_{50}s, efficiency curve parameters, and stokes numbers for MOI calculations

Stage no.	0	1	2	3	4	5	6	7	8	Filter
D_{50}^1, μm	17.5	3.15	1.74	0.98	0.56	0.29	0.175	0.098	0.059	0.28
Slope	6	23	22	22	21	11	11	7.5	4.7	100
Skew	0.0001	0.0001	0.0001	0.0001	0.0001	0.0001	0.0001	0.0001	0.0201	0.0001
$\varepsilon_{\max}$	1	1	1	1	1	1	1	1	1	1
$\varepsilon_{\min}$	0.005	0.002	0.01	0.012	0.005	0.002	0	0	0	1
$(\sqrt{\text{Stk}_{50}})^{1/2}$	0.422	0.528	0.508	0.556	0.559	0.469	0.621	0.576	0.569	1

[1]From fit to calibration data of Marple et al. (1991) using equation of Dzubay and Hasan (1990).
[2]Calculated from Equation (2) using D_{50}s of Marple et al. (1991) determined at 30 L min^{-1}.
[3]Single-stage pressure drop, measured by Marple (1998).
[4]Stokes Number for particle collected with an efficiency of 50%.

According to Marple (1998), the shapes of the efficiency curves for individual stages remain unchanged, for small perturbations in Q and hence D_{50}.

The stage D_{50}s are calculated for the desired flow rate according to

$$D_{50_i} = \sqrt{\frac{\mathrm{Stk}_{50_i} 9\pi N_i \eta D_{jet,i}^3}{4\rho_p Q C_{c_i}}}, \quad [3]$$

where for each of the n stages, Stk_{50}, C_c, and ρ_p are the Stokes number, slip correction, and density of the particle collected with 50% efficiency; N is the number of jets; η is the absolute gas viscosity; and D_{jet} is the jet diameter *for the stage*; and Q is the volumetric flow rate through the impactor (Marple and Willeke 1976). In calculating C_{c_i}s, we assume that the pressure in each impaction region is the stagnation pressure of the stage above, as suggested by Flagan (1982).

The static pressures ($\hat{P}_i$) were calculated for each stage using the dynamic pressure ($P_i^{\blacktriangledown} = {}^1/_2\ \rho_g\ V_{jet_i}^2$, where V_{jet_i} is the gas velocity in the jets of stage i) and the measured barometric pressure (P_{atmos}) according to

$$\hat{P}_i = P_{\mathrm{atmos}} - \sum_{i=0}^{n} P_i^{\blacktriangledown}. \quad [4]$$

To adjust for differences in static pressures calculated with Equation (4) and actual static pressure measurements (Marple et al. 1991) when calculating stage pressures associated with flow rate fluctuations, the measured static stage pressures were regressed against those calculated with Equation (4) with a 4th order polynomial function. *The resulting equation gives what we define as "measurement corrected" static pressures* ($\hat{P}_i^*$):

$$\hat{P}_i^* = 104.9 - 505.5\hat{P}_i + 896.9\hat{P}_i^2 - 994.7\hat{P}_i^3 + 199.4\hat{P}_i^4. \quad [5]$$

In Equation (5) both $\hat{P}_i$ and $\hat{P}_i^*$ are expressed in units of atmospheres.

Values of the Stk_{50} used in our calculations were computed from the corresponding D_{50}s, D_{jet}s, and Ns, published by Marple et al. (1991), and the calculated C_cs for the reference flow rate (30 L min^{-1}).

The mass, M_i, collected on impactor stage i is given as follows:

$$M_i = \sum_{k=1}^{500} M_k \cdot \varepsilon_{k,i} \quad \text{for stage 0} \quad [6a]$$

and

$$M_i = \sum_{k=1}^{500} \left[M_k - \sum_{i=0}^{i=i-1} M_i \right] \cdot \varepsilon_{k,i} \quad \text{for stages } (i)\ 1\text{–}9, \quad [6b]$$

where integrations are over $k = 500$ values of d_p for each stage.

Sample results of the calculations are shown in Figure 1, where we plot the mass collected on each stage at both positive and negative deviations relative to the mass collected at precisely 30 L min^{-1} (true mass) for each stage. As indicated, results are shown for + and − deviations of 0.06, 0.5, 1, 5, and 10% of the reference flow rate (30 L min^{-1}) for an input aerosol with MMAD of 0.5 μm and σ_gs of 1.2, 1.45, and 1.9. As indicated in Figure 1, deviations in mass collected on the various stages were significantly asymmetric with respect to positive and negative deviations in flow rates between 1 and 10% for each of the test distributions, leading to a net mass error even for randomly fluctuating flow rates. Net mass errors, determined as the difference between masses collected at the positive and negative flow rate perturbations of the same amount, are listed in Table 2 for each stage and for each of the flow rate perturbations. In addition, Table 2 contains mass errors for input distributions with an MMAD of 0.2 μm and σ_gs of 1.2, 1.45, and 1.9, i.e., distributions not shown in Figure 1. As indicated in Table 1, the net error in the observed stage masses derived from flow rate fluctuations can be quite substantial, i.e., up to several hundred percent.

For unimodal test aerosol distributions with MMAD of 0.5 μm, the mass ratios peaked on the first stage with $D_{50} >$ 0.5 μm and then tailed off to 1 in either 1 or 2 stages with successively larger D_{50}s, depending on σ_g (see Figure 1). As described above, this is the expected result of the shift in D_{50} caused by the perturbation in flow rate. For D_{50} less than the MMAD of the test aerosol, the ratios increased monotonically with decreasing D_{50} and were largest for the backup filter. The pattern of this behavior was similar for the unimodal 0.2 μm MMAD aerosol cases with the same σ_gs (i.e., 1.2 and 1.45). However, when the test distribution was broadened to a σ_g of 1.9, enough mass was then collected on the 1st and 2nd stages such that mass deviations for the different flow rate perturbations could be observed on these stages as well (see Figure 1).

As indicated in Table 2, the net mass error was smaller for larger values of σ_g, i.e., for broader peaks, and for smaller flow rate fluctuations. Surprisingly, mass errors were larger for MMADs of 0.5 μm than for MMADs of 0.2 μm. As indicated in these tables, the net mass errors were $\leq$1% when flow rate fluctuations were $\leq$1% for all but the most narrow aerosol σ_g, i.e., that of 1.2. From Table 2, it is apparent that flow rate fluctuations would need to be controlled to <0.5% to achieve the 1% net mass error for the most narrow test aerosol. Such narrow distributions have been observed in-stack and in the ambient plume of municipal incinerators (Ondov and Wexler 1998) and may be a common feature of high-temperature combustion sources in which particle growth is dominated by condensation (Biswas et al. 1992).

System for Precision Volumetric Control

The volumetric flow control system consists of a high-precision mass-flow meter (Hastings Instruments, Model HFM 201), proportional control valve (Sierra Instruments, Inc.,

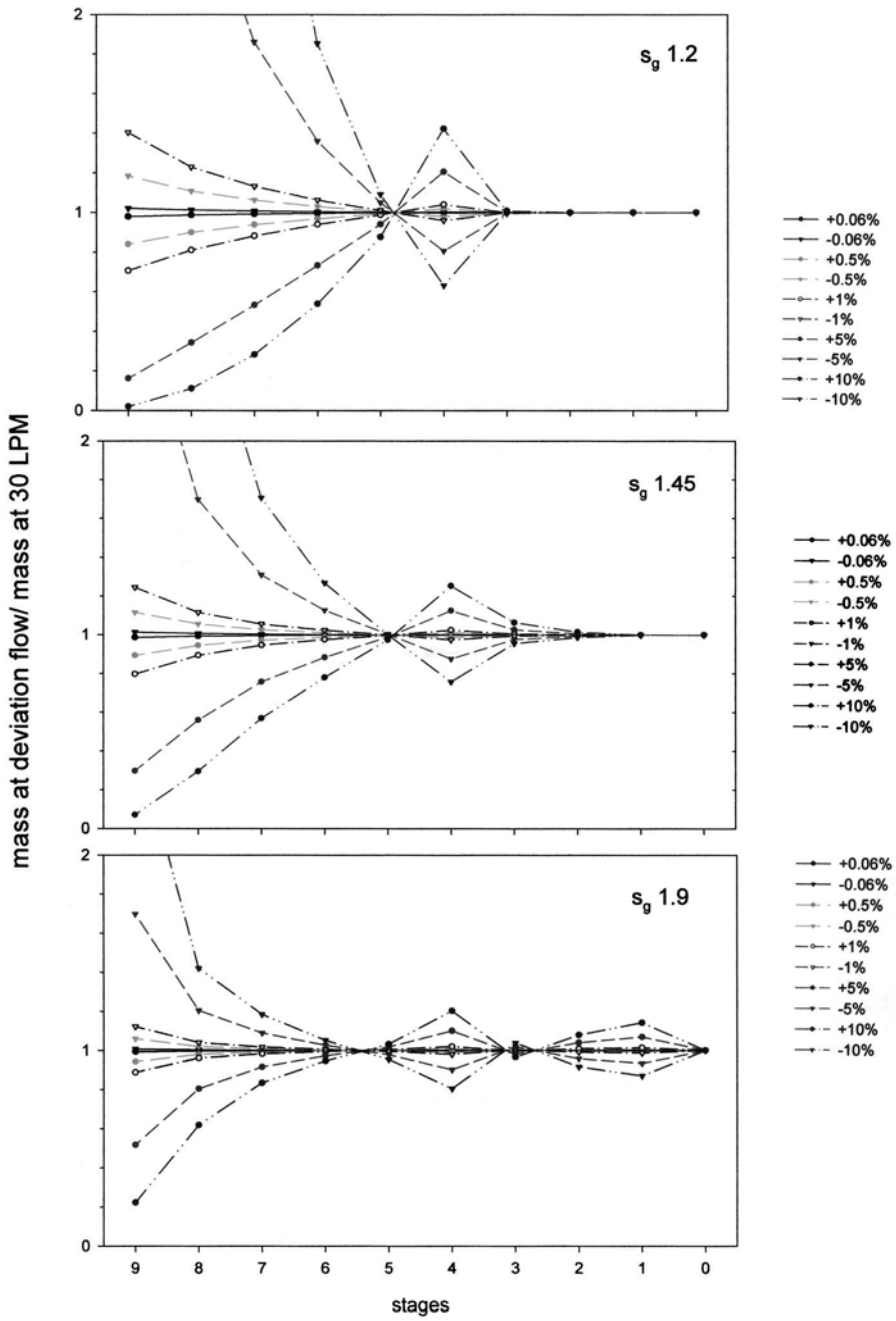

Figure 1. Ratio of mass at perturbed flow rate to mass collected at 30 L min^{-1} for particles with MMAD of 0.5 μm and σ_gs of 1.2, 1.45, and 1.9.

Model 850- L-VO), and microdata logger/computer (Campbell Scientific, Inc., Model CR23X). A capacitance barometer (±0.5 mb precision, Vaisala) and temperature probe (±0.2°C, Campbell Scientific, Inc., Model HMP45C-L11) with a solar radiation shield are used to measure ambient pressure and temperature near the sampler inlet (Figure 2). The mass flow rate is corrected to ambient temperature and pressure in software and an appropriate control signal is generated. The control signal is amplified with a separate precision linear amplifier, designed and built at the University of Maryland, to drive the proportional control valve. The program interrogates the sensors and calculates a new valve setting every 2 s, based on a valve response factor of 10 mV/L min^{-1}. Two systems were constructed.

Performance of the system was observed for several hours in the laboratory and in field sampling, during which time actual flow rates were monitored every 2 s and 1 min averages

Table 2
Percent error in mass collected on MOI stages for various aerosol MMADs and geometric standard deviations at different levels of flow rate fluctuation[1]

MMAD sigma (g)	0.2 μm		0.5 μm		
	1.2	1.45	1.2	1.45	1.9
fluctuation	±0.5%, ±1% , ±5% , ±10%	±0.5%, ±1%, ±5%, ±10%	±0.5%, ±1%, ±5%, ±10%	±0.5%, ±1%, ±5%, ±10%	±0.5%, ±1%, ±5%, ±10%
0, 1	<0.01	<0.01	<0.01	<0.01	<0.01
2	<0.01	<0.01	<0.01	<0.01	<0.01, 0.01, 0.3, 12
3	<0.01	<0.01	<0.01	0.01, 0.02, 0.5, 2	<0.01, <0.01, 0.1, 0.4
4	<0.02	<0.01, <0.01, 0.14, 0.6	0.01, 0.06, 1.4, 5.7	<0.01, 0.1, 0.3, 1.2	<0.01, 0.01, 0.15, 0.6
5	0.05, 0.19, 4.8, 19	0.01, 0.03, 0.8, 3	−0.01, −0.03, −0.73, −2.9	−0.1, −0.02, −0.6, −2.2	<−0.01,−0.01, −0.3, −1.4
6	−.01, −.06, −1.4, −5.4	−0.01, −0.05, −1.2, −4.6	0.1, 0.4, 9.6, 39	0.01, 0.05, 1.3, 5	<−0.01, <−0.01, −0.06, −0.2
7	0.02, 0.07, 1.7, 6.6	0.02, 0.06, 1.5, 5.8	0.4, 1.5, 40, 170	0.07, 0.3, 6.8, 28	<0.01, 0.02, 0.5, 1.9
8	0.3, 1.1, 28, 120	0.1, 0.4, 11, 46	1, 4.2, 110, 560	0.3, 1, 26, 110	0.01, 0.03, 0.9, 4
Bkup	1.4, 5.5, 150, 680	0.3, 1, 26, 110	2.8, 11, 370, 2100	1, 4, 110, 490	0.02, 0.9, 22, 85

[1]For fluctuation of ±0.06% or less, mass errors are <0.2% on all stages except for backup filters.

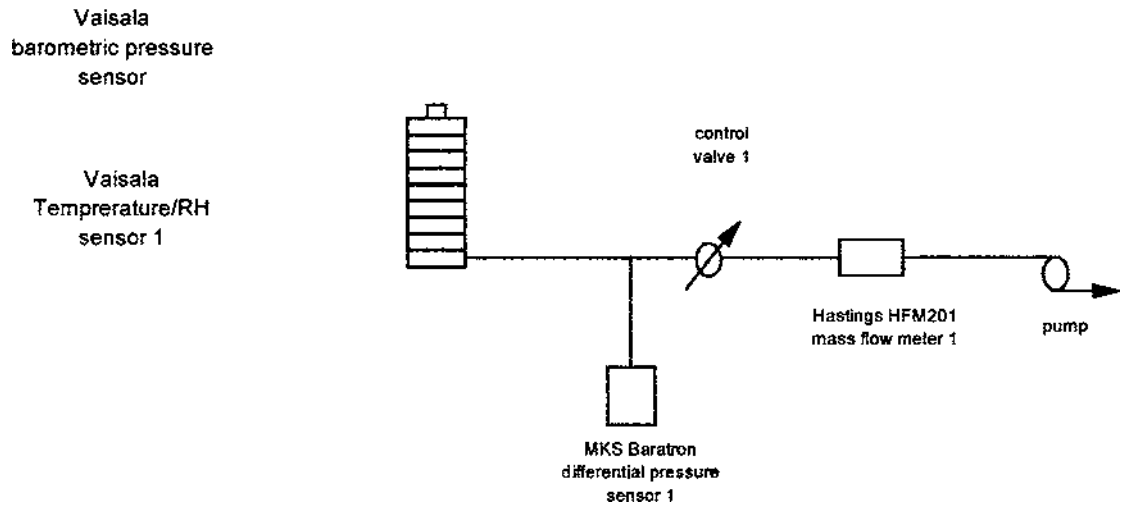

Figure 2. Components of the high-precision flow control system.

were recorded. Results are shown in Figure 3, where we plot controlled and uncontrolled actual volumetric flow rates versus sampling time. Although the pumps used in this study are designed to displace a constant volume of air per unit time, the mass of air displaced changes as the pump heats up or cools, i.e., processes that are affected by ambient temperature and other factors affecting heat transfer, and the volumetric flow rate drawn through the impactor changes accordingly. Changes in ambient pressure can change the leak rate of the pumps; however, this is likely a negligible effect, except perhaps at high altitudes. During the laboratory tests, barometric pressure and temperature changed little, i.e., −0.12% and 0.13%, and −0.92% and −0.2% in both uncontrolled and controlled tests, respectively. During field sampling, variations in barometric pressure and temperature

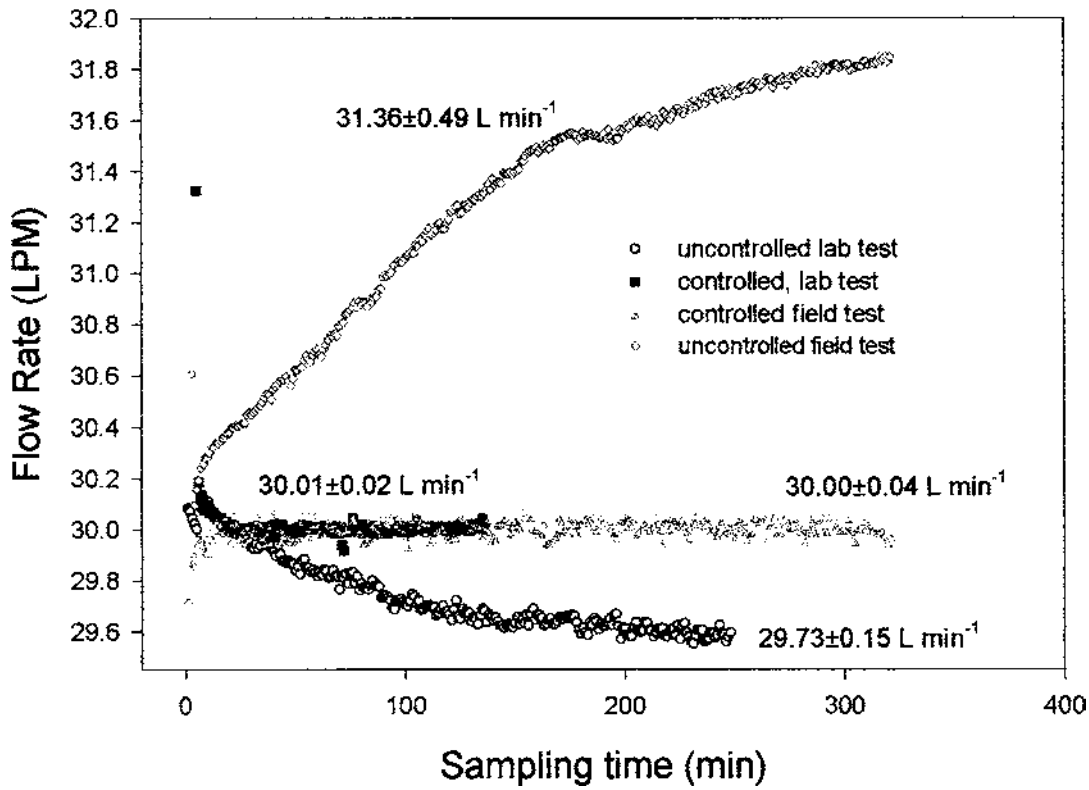

Figure 3. Comparison of flow rates achieved during tests with and without the high-precision flow control system show excellent flow rate regulation.

were somewhat greater than this (i.e., −0.46% and −0.22%; and −4.9% and −2.6% for uncontrolled and controlled tests, respectively). During the controlled (2 h) laboratory test, the actual volumetric flow rate was maintained at an average of 30.0 ± 0.02 L min^{-1}. The flow rate fluctuation (expressed as one standard deviation of the mean) was thus ±0.06%, whereas the flow rate declined steadily during the uncontrolled laboratory test and the average flow rate was 29.73 ± 0.15 L min^{-1}, i.e., a variation of ±0.51% from the mean and a total change in flow rate of 1.7%. In the 5 h field test, the system maintained a volumetric flow rate to within 0.12% (i.e., 30.00 ± 0.04 L min^{-1}) of the preset flow rate. This is a substantial improvement over the ±5.5% variation (from the average) experienced during the uncontrolled field test conducted over a comparable time period, the ±3% (Divita 1993) to ±12% (Howell et al. 1998) flow rate fluctuations experienced in typical field studies using manual or pneumatic flow control methods, and the ±5% fluctuations reported for a commercially available hot wire mass flow controller (Howell et al. 1998).

Mass Errors. Mass errors were estimated for the controlled and uncontrolled field tests by running the impactor model described above using an input aerosol with an MMAD of 0.5 μm and σ_g of 1.2 and the flow rate measurements (321 values) recorded during these tests. In this way, the observed flow rate fluctuations are used rather than random fluctuations. Mass errors were again calculated relative to a 30 L min^{-1} reference flow rate and are plotted against midpoint aerodynamic diameter in Figure 4. As indicated in Figure 3, the distribution of flow rates in the uncontrolled field test are neither random nor symmetric about the average value. Thus larger mass errors are expected relative to the purely random fluctuation cases described above. This is indeed the case. Mass errors were negligible for stages 0, 1, and 2 and small (+0.3%) for stage 3, but were exceptionally large, i.e., +18, −5, −24, −42, −60, and −76%, for the remaining stages. As indicated in panel b of Figure 4, mass errors for the flow controlled test were estimated to be negligible (<0.05%) for all stages, except 7, for which the mass error was only +0.21%. This clearly demonstrates both the necessity for achieving precise flow control when making impactor measurements to determine mass differences and the efficacy of the control system described here.

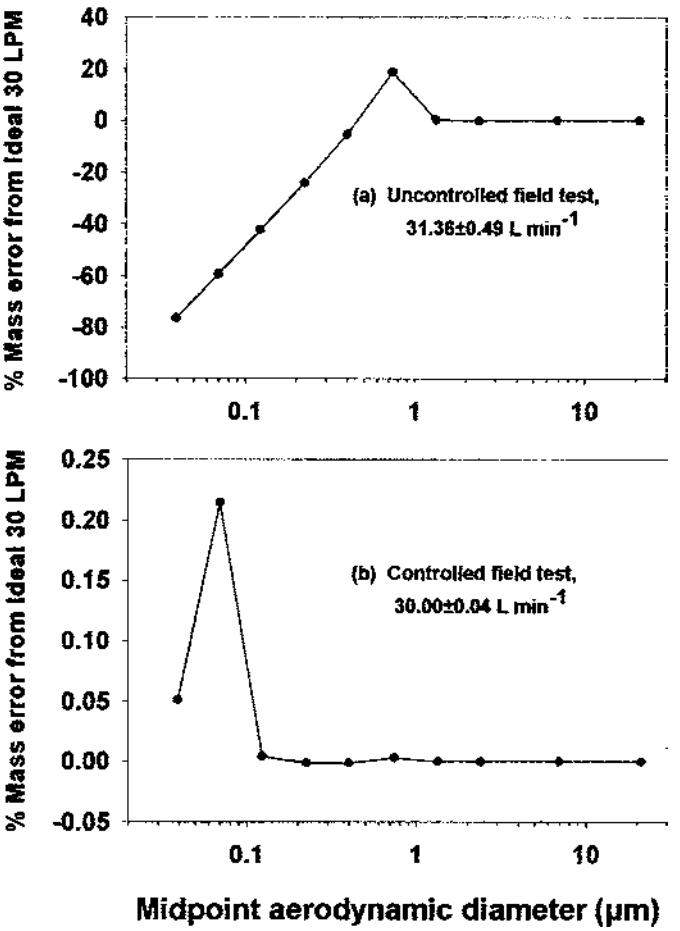

Figure 4. Estimates of mass errors resulting from field operation of uncontrolled (a) and controlled (b) MOIs.

Accuracy Tests

Finally, two tests were run to verify the level of accuracy to which a pair of volumetrically flow controlled MOIs could measure the same test aerosol. In these tests, stage 8 (as specified in Table 1) was removed and a stage with a D_{50} of 6.9 μm (stage A) was installed after the inlet stage. According to Marple (1998), D_{50}s will be identical for two MOI stages of the same design and with identical pressure drops. However, small differences in pressure drops can be expected due to small differences in jet diameters. Individual pressure drops across stages 4–7 of two nominally-identical 9 stage MOIs were determined by Marple (1998). Those across stages 4 and 5 were identical (13.39 and 14.79 mbar for impactors B and BB, respectively), whereas those for stages 6 and 7 differed slightly (i.e., 35.73 and 36.14 mbar for stage 6 of impactor B and BB, respectively, and 83.24 and 82.72 mbar for stage 7 of these respective impactors). As indicated pressure drops corresponding to individual stages differed by no more than 1.1%. Thus by virtue of Equations (3)–(5), D_{50}s were expected to deviate by no more than 0.2%, which corresponds to a 0.4% change in the interval width. If mass were distributed uniformly with respect to the sizes of particles collected on such a stage, then a 0.4% change in interval width would produce a 0.4% change in the mass collected and thus, if undetected, a 0.4% error in mass collected. However, particle mass is not distributed uniformly with respect to the sizes of particles collected in the various intervals, and this can lead to a substantial magnification effect. For example, the difference in the integral of the LNDF over the interval 0.55–1 μm versus 0.55/1.002 to 1 μm (i.e., a difference in the lower D_{50} of 0.2%) would be 5.9% for an MMAD and σ_g of 0.2 μm and 1.2, respectively. However, this difference drops to 1.5% for a σ_g of 1.45 and to 0.6% for a σ_g of 1.9. Clearly and understandably, it is difficult to accurately measure such narrow aerosol distributions with a relatively low resolving power of the MOI.

One of the mass flow meters (i.e., HFM-1) of the two control systems was supplied with an 11 point NIST-traceable calibration, and its reported accuracy was 0.075% (indicated flow was 39.97 L min^{-1}) at 40.00 L min^{-1}. The second mass flow meter (HFM-2) was calibrated against the first in our laboratory over the range 0 to 30 L min^{-1} in 19 100 mV increments, recorded on a CR23X data logger. Linear regression coefficients of the output signal, i.e., in mV, from HFM-02 against the indicated flow of HFM-1, the reference meter, were 11.8513 $\pm$ 0.0181 mV/L min^{-1}, 1.998 $\pm$ 0.392 L min^{-1}, and 0.999960 for the slope, intercept, and R^2, respectively. The accuracy, i.e., defined as the root-mean-square-deviation between the two meters, is therefore $\pm$0.19%. According to our model calculations, the differences between masses collected on MOI stages 4–7 corresponding to a +0.19% bias (not fluctuation) in flow rates (i.e., 30.00 versus 30.06 L min^{-1}) could be <3% for an aerosol with a MMAD of 0.2 μm and σ_g of 1.2.

In the accuracy tests, 0.209 $\pm$ 0.01 μm diameter, monodisperse, unit density fluorescent particles (Polysciences, Model 40) were dispersed with a laboratory 2-fluid nebulizer (De Vilbiss

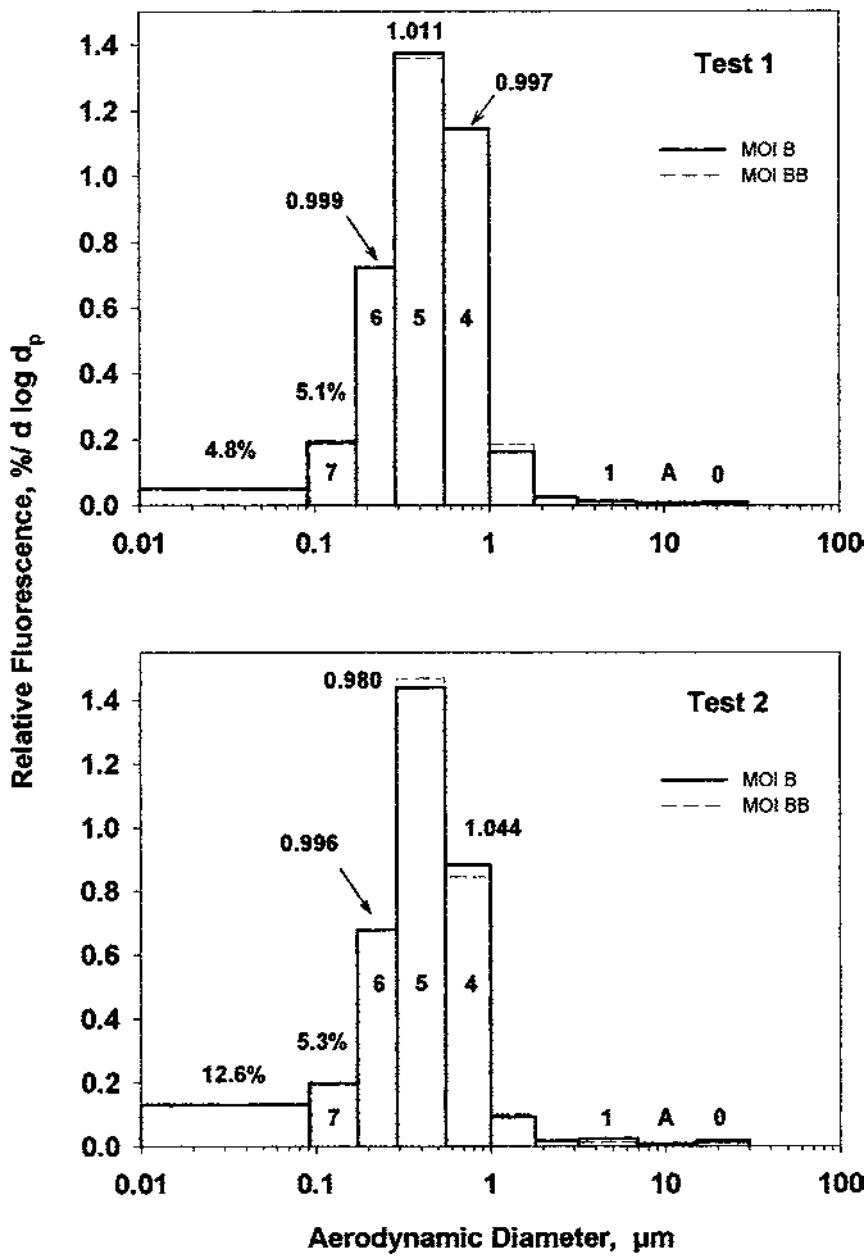

Figure 5. Test aerosol spectra collected with 2 simultaneously operated MOIs. Stages 0, A, 1, and 4–7 are labeled, as are percentages of fluorescence collected on stages 8 and 9 and ratios of fluorescence measured on stages of impactors B and BB.

Model 40) with a 10 L min^{-1} flow of filtered, dry nitrogen metered with a mass flow meter (Aalborg). The test aerosol was dried in a 2 L chamber and discharged to Boltzmann equilibrium by exposure to beta emissions from three ^{85}Kr sources. The two MOIs were connected to a precisely-machined symmetric plenum (University Research Glassware, Carboro, NC) and used to sample the test aerosol for 60 min, after which the positions of the MOIs were exchanged and sampling was continued for an additional 60 min. The test was then repeated. Flow rates of the 2 impactors, herein designated B and BB, were 30.01 ± 0.04 (B) and 30.01 ± 0.02 (BB) L min^{-1}, respectively, in the first test and 30.01 ± 0.04 (B) and 30.01 ± 0.03 (BB) L min^{-1}, respectively, in the second test. After sampling, each of the impaction stages (37 mm Nuclepore polycarbonate films) were extracted with a 10.00 ± 0.02 mL aliquot of ethyl acetate and the fluorescence intensity measured on an Aminco Bowmen Series 2 Luminescence Spectrometer at an excitation wavelength of 440 nm by integrating light emitted between 450 and 600 nm.

In the absence of particles consisting of multiple numbers of the monodisperse test particles, most of the mass of test particle mass would be collected on stage 6, whose D_{50} is 0.173 μm. A simulation with the Monte-Carlo model was made using the test particle distribution and measured flow rate of 30.01 ± 0.04 L min^{-1}. The model was run 500 times, randomly choosing Gaussian values of particle diameter for a normal distribution of input particles with the 0.209 μm mean and 0.01 μm standard deviation. The results suggest that, without multiples, 82% of the mass of these particles would have been collected on stage 6, 11.5% on stage 7, and 0.02% on the backup filter. As indicated in Figure 5, however, most of the 0.2 μm particle mass was collected on stage 5 (D_{50} 0.29 μm), indicating a large fraction of doublets and/or substantial residue from the water used to disperse the particles. As indicated in Figure 5, only 5.1% (5.3% in test 2), i.e., about half of the ideal amount, was collected on stage 7, presumably due to reduction in the single particle concentration due to multiplet formation. As only 0.02% of the test particle mass should have reached the backup filter, we can attribute virtually all of the backup filter mass (i.e., 4.8 and 12.6%) for both tests to particle bounce. Clearly this represents a worst case in that dry solid test particles were used on flat, uncoated substrates. In sampling ambient submicrometer aerosol, less bounce would be expected.

Nevertheless, very good agreement was observed for the 2 impactors, i.e., the amounts collected on stages 4, 5, and 6 of the 2 impactors differed by only 0.1, 1.1, and 0.3%, respectively, in the first test and by 4, 2, and 0.4% in the second test. This is quite good considering that the uncertainty in the wash volumes was about $\pm 0.2\%$ and the flow rate bias error could have led to an uncertainty of as much as 3%.

The fact that the second test showed poorer agreement than the first test could be an indication of jet clogging. This suggests that precise measurements would require cleaning and new pressure drop measurements to be made on stages with small jet diameters before and after each use of the impactor.

CONCLUSIONS

Calculations using the MOI efficiency curves show that mass error associated with flow rate fluctuations can be expected to be $<1\%$ for all impaction stages when flow rate fluctuations are maintained below 0.5%. Mass errors for backup filters are expected to be somewhat larger (up to 3%), but can be less than or comparable to backup filter mass error due to particle bounce, depending on the type and condition of impaction substrates and the nature of the aerosol. This level of control is reasonably achieved with the readily-constructed flow control system described above.

REFERENCES

Ahlberg, M. S., and Winchester, J. W. (1978). Dependence of Aerosol Sulfur Particle Size on Relative Humidity, *Atmos. Environ.* 12:1631–1632.

Annegarn, H. J., Leslie, A. C. D., Winchester, J. W., and Sellchop, J. P. F. (1983). Particle Size and Temporal Characteristics of Aerosol Composition Near Coal-Fired Electric Power Plants of the Eastern Transvaal, *Aerosol Sci. Technol.* 2:489–498.

Berner, A., Sidla, S., Galambos, Z., Kruisz, C., Hitzenberger, R., ten Brink, H. M., and Kos, G. P. A. (1996). Modal Character of Atmospheric Black Carbon Size Distributions, *J. Geophys. Res.* 101:19,559–19,565.

Biswas, P., Lin, W. Y., and Wu, C. Y. (1992). *Formation and Emission of Metallic Aerosols from Incinerators*, Proceedings of the 1992 European Aerosol Conference, Oxford.

Caffrey, P. F. (1997). Measurement of Fine-Particle Dry Deposition to Lake Michigan. Ph.D. Thesis, University of Maryland, College Park.

Caffrey, P. F., Ondov, J. M., Zufall, M. J., and Davidson, C. I. (1998). Determination of Size-Dependent Dry-Particle Deposition Velocities with Multiple Intrinsic Elemental Tracers, *Environ. Sci. Technol.* 32:1615–1622.

Cushing, K. M., McCain, J. D., and Smith, W. B. (1979). Experimental Determination of Sizing Parameters and Wall Losses of Five Source-Test Cascade Impactors, *Environ. Sci. Technol.* 13:726–731.

Divita, F., Suarez, A., Ondov, J. M., and Suarez, A. (1995). Size Spectra and Hygroscopic Growth of Particles Bearing As, Se, Sb, and Zn in College Park Aerosol, *J. Radio. Nuc. Chem.* 192:215–228.

Divita, Jr., F. (1993). *Characterization and Sources of Atmospheric Submicrometer Particles in Washington, D.C. and Philadelphia, PA,* Ph.D. thesis, University of Maryland, College Park, MD, December.

Divita, Jr., F., Ondov, J. M., and Suarez, A. E. (1996). Size-Spectra and Atmospheric Growth of V-Containing Aerosol in Washington, D.C., *Aerosol Sci. Technol.* 25:256–273.

Dzubay, T. G., and Hasan, H. (1990). Fitting Multimodal Lognormal Size Distributions to Cascade Impactor Data, *Aerosol Sci. Technol.* 13:144–150.

Dzubay, T. G., Hines, L. E., and Stevens, R. K. (1976). Particle Bounce Errors in Cascade Impactors, *Atmos. Environ.* 10:229–234.

Fegley, M. J., and Ensor, D. S. (1975). *The Propagation of Errors in Particle Size Distribution Measurements Performed Using Cascade Impactors,* Paper No. 75-32.5, 68th Annual Meeting of the Air Pollution Control Association, Boston, MA, June 15–20.

Flagan, R. C. (1982). Compressible Flow Inertial Impactors, *J. Colloid Interface Sci.* 87:291–299.

Hasan, H., and Dzubay, T. G. (1987). Size Distributions of Species in Fine Particles in Denver Using a Microorifice Impactor, *Aerosol Sci. Technol.* 6: 29–39.

Hering, S. V., and Friedlander, S. K. (1982). Origins of the Aerosol Sulfur Size Distributions in the Los Angeles Basin, *Atmos. Environ.* 16:2647–2656.

Hitzenberger, R., Berner, A., Dusek, U., and Alabashi, R. (1997). Humidity-Dependent Growth of Size-Segregated Aerosol Samples, *Aerosol Sci. Technol.* 27:116–130.

Hoff, J., Borgoul, P., Ondov, J. M., Kelly, W. R., and Chen, L. T. (1998). Feasibility of Applying a New Tracer for Direct Determination of Dry Particulate Deposition, *J. Air and Waste Managem.* 48:721–728.

Howell, S., Pszenny, A. A. P., Quinn, P., and Huebert, B. (1998). A Field Intercomparison of Three Cascade Impactors, *Aerosol Sci. Technol.* 29:475–492.

John, W., Wall, S. M., Ondov, J. L., and Winklmayr, W. (1990). Modes in the Size Distributions of Atmospheric Inorganic Aerosol, *Atmos. Environ.* 24A: 2349–2359.

Koutrakis, P., Wolfson, J. M., Spengler, J. D., Stern, B., and Franklin, C. A. (1989). Equilibrium Size of Atmosphreic Aerosol Sulfates as a Function of the Relative Humidity, *J. Geophys. Res.* 94:6442–6448.

Kuhlmey, G. A., Liu, B. Y. H., and Marple, V. A. (1981). A Micro-Orifice Impactor for Sub-Micron Aerosol Size Classification, *Am. Ind. Hyg. Assoc. J.* 42:790–795.

Lin, J. J., Noll, K. E., and Holsen, T. M. (1994). Dry Deposition Velocities as a Function of Particle Size in the Ambient Atmosphere, *Aerosol Sci. Technol.* 20:239–252.

Marple, V. A. (1998). *Personal Communication*, University of Minnesota, Minneapolis, MN.

Marple, V. A., Liu, B. Y. H., and Kuhlmey, G. A. (1981). A Uniform Deposit Impactor, *J. Aerosol Sci.* 12:333–337.

Marple, V. A., Rubow, K. L., and Behm, S. M. (1991). A Microorifice Uniform Deposit Impactor (MOUDI): Description, Calibration, and Use, *Aerosol Sci. Technol.* 14:434–446.

Marple, V. A., and Willeke, K. (1976). Impactor Design, *Atmos. Environ.* 10:891–896.

May, K. R. (1945). The Cascade Impactor: An Instrument for Sampling Coarse Aerosols, *J. Sci. Instr.* 22:187–195.

McMurry, P. H., and Wilson, J. C. (1983). Droplet Phase (Heterogeneous) and Gas Phase (Homogeneous) Contribtuions to Secondary Ambient Aersosol Formation as Functions of Relative Humidity, *J. Geophys. Res.* 88: 5101–5108.

Natusch, D. F. S., and Wallace, J. R. (1976). Determination of Airborne Particle Size Distributions: Calculation of Cross-Sensitivity and Discreteness Effects in Cascade Impaction, *Atmos. Environ.* 10:315–324.

Nurtan, A. E., Ziegler, P., and Whitfield, R. (1978). The Adhesion of Particles Upon Impaction, *J. Aerosol Sci.* 9:547–556.

Ondov, J. M., and Divita, F. (1993). Size Spectra for Trace Elements in Urban Aerosol Particles by Instrumental Neutron Activation Analysis, *J. Radio. Nuc. Chem.* 167:247–258.

Ondov, J. M., Ragaini, R. C., and Biermann, A. H. (1978). Elemental Particle-Size Emissions from Coal-Fired Power Plants: Use of an Inertial Cascade Impactor, *Atmos. Environ.* 12:1175–1185.

Ondov, J. M., and Wexler, A. S. (1998). Where Do Particulate Toxins Reside? An Improved Paradigm for the Structure and Dynamics of the Urban Mid-Atlantic Aerosol, *Environ. Sci. Technol.* 32:2547–2555.

Paode, R. D., Sofuoglu, S. C., Sivadechathep, J., Noll, K. E., Holsen, T. H., and Keeler, G. J. (1998). Dry Deposition Fluxes and Mass Size Distributions of Pb, Cu, and Zn Measured in Southern Lake Michigan during AEOLOS, *Environ. Sci. Technol.* 32:1629–1635.

Raabe, O. G. (1978). A General Method for Fitting Size Distributions to Multicomponent Aerosol Data Using Weighted Least-Squares, *Environ. Sci. Technol.* 12:1162–1167.

Rao, A. K., and Whitby, K. T. (1978). Non-Ideal Collection Characteristics of Inertial Impactors—II. Cascade Impactors, *J. Aerosol Sci.* 9:87–100.

Venkataraman, C., and Friedlander, S. K. (1994). Size Distributions of Polycyclic Aromatic Hydrocarbons and Elemental Carbon. 2. Ambient Measurements and Effects of Atmospheric Processes, *Environ. Sci. Technol.* 28:563–572.

Wolfenbarger, J. K., and Seinfeld, J. H. (1990). Inversion of Aerosol Size Distribution Data, *J. Aerosol Sci.* 21:227–247.